J|A|C|S
ARTICLES

Published on Web 10/21/2010

Fluorescence Resonance Energy Transfer in Gaseous, Mass-Selected Polyproline Peptides

Francis O. Talbot, Anthony Rullo, Huihui Yao, and Rebecca A. Jockusch*

Department of Chemistry, University of Toronto, Toronto, ON M5S 3H6, Canada

Received July 29, 2010; E-mail: rebecca.jockusch@utoronto.ca

Abstract: Despite the many successes of mass spectrometry in the analysis of biological samples, the need to better understand the correlation between condensed-phase properties and those of electrospray species remains. In particular, the link between structures in the condensed phase and in the gaseous environment of the mass spectrometer is still elusive. Here, we show that fluorescence resonance energy transfer (FRET) can be used to probe the conformations of gaseous biopolymers which are formed by electrospray ionization (ESI) and manipulated in a quadrupole ion trap mass spectrometer. A rhodamine dye pair suitable for gas-phase FRET is characterized. Both steady state spectra and lifetime measurements are used to monitor energy transfer in a series of dye-labeled polyproline-based peptides. FRET efficiency is explored as a function of peptide chain length and charge state. For the peptide with eight proline repeats, virtually complete energy transfer is observed. For the peptide with 14 proline repeats, energy transfer decreases as the charge state increases, consistent with Coulomb repulsion induced elongation of the peptide backbone. FRET measurements of the longest peptide examined, which has 20 proline repeats, indicates that the peptide adopts a bent configuration. Evidence for multiple conformations present within the ensemble of trapped ions is provided by fluorescence lifetime measurements. Gas-phase FRET measurements promise to be a new route to probe the conformations of large gaseous ions.

Introduction

Fluorescence resonance energy transfer (FRET) is a sensitive probe of molecular structure that is now widely used in the biological sciences. In FRET, the energy transfer from an excited donor fluorophore to a nearby acceptor depends strongly (inverse sixth power) on the distance between these two fluorophores, making the technique ideal for probing distances in the range 3−8 nm.[1,2] This sensitivity to distances at a scale that matches well the sizes of large biomolecular species has allowed scientists to study a wide variety of biochemical processes, including protein folding,[3−5] and promoted considerable advances in cellular imaging in the condensed phase.[6,7] Concomitantly, major advances in soft vaporization and ionization sources[8−10] have rendered mass spectrometry (MS) tools and techniques increasingly popular for bioanalysis in the last two decades. The highly controlled environment of the mass spectrometer allows sophisticated investigations of molecular systems, ranging in size from diatomics up to megadalton complexes, providing insight into their composition, stoichiometry, and structure.[11] It should be emphasized that MS analysis is ultimately performed in the gas phase. Thus, it can provide information about the intrinsic properties of isolated molecules, complementary to that obtained from condensed-phase experiments. However, MS is often employed as a tool to investigate solution-phase properties of biomolecules and their complexes. A better understanding of the relationship between the properties of biomolecules in the condensed phase and those present in the mass spectrometer will aid reliable interpretation of MS data. Here, we present results obtained using FRET to probe the conformation of gaseous peptides stored and manipulated in a mass spectrometer.

While powerful techniques such as nuclear magnetic resonance (NMR) and X-ray crystallography can be used to determine the conformation of large molecules such as proteins in the condensed phase, no gas-phase equivalent is available, and much less is known about the structures of large gaseous molecules. Pieces of the conformational puzzle of gaseous molecules have come from predominantly ion mobility, dissociation, and reactivity based (for example, gas-phase hydrogen−deuterium exchange) experiments.[11−19] Of these, interpretation of data from ion mobility based devices, which include

(1) Lakowicz, J. R. *Principles of Fluorescence Spectroscopy*; Springer: New York, 2006.
(2) Förster, T. *Ann. Phys.* **1948**, *437*, 55–75.
(3) Muñoz, V. *Annu. Rev. Biophys. Biomol. Struct.* **2007**, *36*, 395–412.
(4) Royer, C. A. *Chem. Rev.* **2006**, *106*, 1769–1784.
(5) Schuler, B.; Lipman, E. A.; Eaton, W. A. *Nature* **2002**, *419*, 743–747.
(6) Dehmelt, L.; Bastiaens, P. I. H. *Nat. Rev. Mol. Cell Biol.* **2010**, *11*, 440–452.
(7) Rao, J.; Dragulescuandrasi, A.; Yao, H. *Curr. Opin. Biotechnol.* **2007**, *18*, 17–25.
(8) Fenn, J.; Mann, M.; Meng, C.; Wong, S.; Whitehouse, C. *Science* **1989**, *246*, 64–71.
(9) Wilm, M.; Mann, M. *Anal. Chem.* **1996**, *68*, 1–8.
(10) Karas, M.; Bachmann, D.; Bahr, U.; Hillenkamp, F. *Int. J. Mass Spectrom. Ion Process.* **1987**, *78*, 53–68.
(11) *Principles of Mass Spectrometry Applied to Biomolecules*; Laskin, J., Lifshitz, C., Eds.; John Wiley and Sons: New York, 2006.
(12) Polfer, N.; Oomens, J. *Mass Spectrom. Rev.* **2009**, *28*, 468–494.
(13) Bohrer, B. C.; Merenbloom, S. I.; Koeniger, S. L.; Hilderbrand, A. E.; Clemmer, D. E. *Annu. Rev. Anal. Chem.* **2008**, *1*, 293–327.
(14) Benesch, J. L.; Robinson, C. V. *Curr. Opin. Struct. Biol* **2006**, *16*, 245–251.
(15) Jarrold, M. F. *Annu. Rev. Phys. Chem.* **2000**, *51*, 179–207.

10.1021/ja1067405

drift tubes, traveling wave devices, differential mobility analyzers, and high-field asymmetric ion mobility separators, is often the most straightforward. Most well-developed among these are drift tube ion mobility experiments, which can separate conformers and provide collisional cross sections differing by ~1%.[20] A significant advantage of ion mobility is that basic data interpretation is relatively straightforward. However, with these experiments, structural information is underdetermined (a single parameter is obtained); modeling must be used to make the link to detailed structure.

Laser spectroscopy is a particularly sensitive probe of molecular structure, as it allows direct probing of the vibrational modes of a molecule. In the infrared, for example, the vibrational absorption transition associated with some selected chemical bonds is extremely sensitive to the immediate environment of that bond, providing information about local molecular structure.[21] Over the last 5 years, action spectroscopy using tunable IR lasers to fragment mass-selected ions has been especially popular and provided a wealth of data about the conformational landscapes of small systems, including biological building blocks, short oligomers, and small complexes.[12] IR action spectra of longer peptides[22−25] and proteins[26] have also been measured; however, interpretation of the IR spectra of larger systems such as proteins is challenging, due to both spectral congestion (many overlapping bands) and to computational difficulties arising from complexity of the conformational landscape and the current unfavorable scaling with molecular size of the computational methods usually employed to aid data analysis. While spectral resolution can be improved by cooling,[22] the difficulties associated with computation of large systems remain. Thus, the amount of useful structural information gained from infrared spectra is considerably reduced as the size of the molecule increases. Furthermore, fragmentation generally becomes increasingly difficult with molecular size, leading to reduced signal. On the other hand, as the molecules under study get larger (several dozens of amino acids and more), they reach sizes that are particularly well-suited for investigations using a technique like FRET. Moreover, the sensitivity of fluorescence is not affected by molecular size.

To date, FRET measurements have been performed almost exclusively in the condensed phase. One reason for this is that FRET is most efficiently applied to molecular systems several nanometers in dimension, in particular biologically relevant ones. Techniques developed as ion sources for mass spectrometry, such as electrospray ionization (ESI)[8] and matrix-assisted laser desorption ionization (MALDI),[10] allow transfer of large biomolecules from solution intact into the gas phase. Recently, several research groups have developed instruments to perform fluorescence measurements on gaseous ions formed by ESI and MALDI and stored and manipulated in trapping mass spectrometers.[27−31]

The controlled environment of a mass spectrometer offers several advantages. It allows the examination of the intrinsic conformational preferences of the molecules under study; solvent molecules can then be added stepwise, in a controlled manner, in order to determine their effect. Another advantage of the mass spectrometer is the ability to isolate one unique mass-to-charge species for targeted investigation, thereby eliminating almost completely one of the main sources of error in condensed-phase FRET, which is the potential presence, in the sampled volume, of partially labeled molecules. The fluorescence signal from molecules labeled with only the donor fluorophore increases the intensities of the donor band and can lead to erroneous estimations of energy transfer.[1] Because of such biases, it is often more reliable to use the measurements of fluorescence lifetimes of the donor for the estimation of energy transfer. But even lifetimes measurements can be affected by sample heterogeneity as the absence of observed transfer (unchanged lifetime for the donor) is consistent with either a long distance between fluorophores or the total absence of acceptor (i.e., partially labeled molecules). In order to alleviate these shortcomings in cases of low transfer efficiencies, Kapanidis et al. developed a new variant of FRET, called *al*ternating *ex*citation FRET (ALEX-FRET).[32] Here, a second laser beam tuned to an absorption band of the acceptor is used, in a confocal setup and at the single molecule limit, in order to establish the presence of both fluorophores on the molecular system being observed. By contrast, in the mass spectrometer, the singly tagged peptides appear at a different mass-to-charge than the doubly (donor and acceptor) tagged ones and can be easily ejected from the ion storage area, leaving only the desired species. Additionally, the presence in the mass spectra of multiple charge states for the peptides (a feature of electrospray ionization with molecules of moderate to large sizes) offers the unique opportunity to study the influence of charge states on the conformation of a given molecule or the effect on fluorescence of charges in the vicinity of the dye.

We use a model system based on polyproline peptides. These were employed in seminal work by Stryer and Haugland, who presumed them to be rigid helices ("molecular rulers"), illustrating the distance dependence of FRET in biomolecules for the first time in the condensed phase.[33] More recently, the use of these polyproline peptides as "molecular rulers" in FRET has been revisited, using single molecule spectroscopy and computations; marked deviations from the expected rigid structure

(16) Wood, T.; Chorush, R.; Wampler, F.; Little, D.; O'Connor, P.; McLafferty, F. *Proc. Natl. Acad. Sci. U.S.A* **1995**, *92*, 2451–2454.
(17) McLuckey, S.; Goeringer, D. *J. Mass Spectrom.* **1997**, *32*, 461–474.
(18) Valentine, S. J.; Kurulugama, R. T.; Bohrer, B. C.; Merenbloom, S. I.; Sowell, R. A.; Mechref, Y.; Clemmer, D. E. *Int. J. Mass Spectrom.* **2009**, *283*, 149–160.
(19) *Modern Mass Spectrometry*; Schalley, C. A., Ed.; Springer Berlin Heidelberg: Berlin, 2003; Vol. 225.
(20) Kemper, P.; Dupuis, N.; Bowers, M. *Int. J. Mass Spectrom.* **2009**, *287*, 46–57.
(21) Eyler, J. *Mass Spectrom. Rev.* **2009**, *28*, 448–467.
(22) Nagornova, N.; Rizzo, T.; Boyarkin, O. *J. Am. Chem. Soc.* **2010**, *132*, 4040–4041.
(23) Kupser, P.; Pagel, K.; Oomens, J.; Polfer, N.; Koksch, B.; Meijer, G.; von Helden, G. *J. Am. Chem. Soc.* **2010**, *132*, 2085–2093.
(24) Pagel, K.; Kupser, P.; Bierau, F.; Polfer, N.; Steill, J.; Oomens, J.; Meijer, G.; Koksch, B.; von Helden, G. *Int. J. Mass Spectrom.* **2009**, *283*, 161–168.
(25) Stearns, J. A.; Boyarkin, O. V.; Rizzo, T. R. *J. Am. Chem. Soc.* **2007**, *129*, 13820–13821.
(26) Oomens, J.; Polfer, N.; Moore, D. T.; van der Meer, L.; Marshall, A. G.; Eyler, J. R.; Meijer, G.; von Helden, G. *Phys. Chem. Chem. Phys.* **2005**, *7*, 1345.
(27) Bian, Q.; Forbes, M. W.; Talbot, F. O.; Jockusch, R. A. *Phys. Chem. Chem. Phys.* **2010**, *12*, 2590–2598.
(28) Wang, Y.; Hendrickson, C.; Marshall, A. *Chem. Phys. Lett.* **2001**, *334*, 69–75.
(29) Khoury, J.; Rodriguez-Cruz, S.; Parks, J. *J. Am. Soc. Mass Spectrom.* **2002**, *13*, 696–708.
(30) Frankevich, V.; Guan, X.; Dashtiev, M.; Zenobi, R. *Eur. J. Mass Spectrom.* **2005**, *11*, 475–482.
(31) Sassin, N.; Everhart, S.; Dangi, B.; Ervin, K.; Cline, J. *J. Am. Soc. Mass Spectrom.* **2009**, *20*, 96–104.
(32) Lee, N. K.; Kapanidis, A. N.; Wang, Y.; Michalet, X.; Mukhopadhyay, J.; Ebright, R. H.; Weiss, S. *Biophys. J.* **2005**, *88*, 2939–2953.
(33) Stryer, L.; Haugland, R. P. *Proc. Natl. Acad. Sci. U.S.A.* **1967**, *58*, 719–726.

of these peptides were found.[34−36] Polyprolines have also been studied in the gas phase. Parks and co-workers have examined the conformational flexibility in peptides with up to 10 proline repeats using fluorescence contact quenching measurements and found these to be rigid at room temperature.[37] Counterman and Clemmer used ion mobility to show that polyprolines can adopt multiple conformations in the gas phase, when sprayed from water/methanol/acetic acid solution. The measured collisional cross sections indicated the presence of both extended and somewhat more compact conformations, with more highly charged peptides adopting more extended conformations. Evidence of folding in some longer polyproline chains was also found.[38]

Implementing FRET measurements inside a mass spectrometer has proven challenging. This is due to both the low density of gaseous ions and limited optical access to the fluorescing ions. To date, only two groups have been successful in detecting FRET signal from gaseous molecular ions.[39,40] In both studies, a decrease in total fluorescence signal from the donor dye was measured in the presence of an acceptor, providing evidence that FRET was taking place. Unfortunately, no estimation of FRET efficiency could be obtained from either set of data. Here, we report on the first measurements of FRET efficiencies in the gas phase, using both spectral and temporal (lifetimes) measurements.

Experimental Section

Mass Spectrometry and Spectroscopy. Experiments were performed on an Esquire 3000+ quadrupole ion trap (QIT, Bruker Daltonik, Bremen, Germany) that has been modified to perform photodissociation action spectroscopy and laser-induced fluorescence of trapped ions. A full description of the modifications is available elsewhere.[27,41]

Molecular ions were generated by electrospray ionization from 50:50 (v:v) water:methanol solvent. The desired ions were mass-selected and stored in the trapping region of the QIT, where they were irradiated with laser light. The total number of ions trapped is reflected by the ion charge control (ICC) parameter provided in the Bruker software. Typical ICC values for stored ions in these experiments varied in the range $(2-10) \times 10^5$, depending on sample quality and abundance of the desired charge state. The number of ions in the trap is estimated to be $^1/_{20}$ of the ICC.

The laser light was the doubled output of a mode-locked Ti:sapphire (Tsunami, Spectra-Physics, Mountain View, CA) providing pulses of ∼130 fs fwhm and 2−22 nJ energy at 80 MHz repetition rate. The IR light is frequency tunable from 700 to 1070 nm, yielding, upon second harmonic generation (SHG), visible light in the range 350−535 nm with powers ranging from 2 to 200 mW. Control of the irradiation timing is effected by using a trigger from the QIT to control a mechanical shutter placed in the laser beam's path. The ions were typically irradiated with 6−20 mW at 470 or 510 nm wavelength. A small portion of the fluorescence is collected orthogonally to the path of the excitation beam and passes a sharp cutoff long-pass or band-pass filter (Chroma Technology Corp., Rockingham, VT and Semrock, Rochester, NY) to further eliminate scattered laser light and/or isolate a particular portion of the fluorescence spectrum. For steady-state fluorescence measurements, the fluorescence emission is focused onto the slit of a spectrograph (Shamrock 303i) equipped with an electron-multiplying charge coupled device (EM-CCD) camera (Newton), both from Andor Technologies (Belfast, Ireland). The EM-CCD is cooled to −75 °C, and exposure times ranged from 2 to 10 s. In all cases, the recorded mass spectra showed no significant fragmentation at the combination of laser power and irradiation time used. The fluorescence spectra shown correspond to the signal obtained over a total of ∼1000 s, which was obtained by measuring 100−500 different ion populations. All spectra were normalized by laser power, irradiation time, and ICC. However, the largest uncertainty in the normalization used is the relation between recorded ICC and the actual number of trapped ions. In particular, the ICC value might exhibit a dependence on the charge state of the detected species; this issue requires additional investigation.

For lifetime measurements, the (filtered) fluorescence light was diverted toward an infinity-corrected objective (RMS10X, Thorlabs, Newton, NJ) which focused it onto a single-photon avalanche diode (PDM series, 100 μm diameter active area) from Micro Photon Devices. Concurrently, the laser beam exiting the QIT was sent onto a fast photodiode (DET10A, Thorlabs, Newton, NJ), and the signals from both detectors (SPAD and photodiode) were sent to a time correlated single photon counting (TCSPC) card, model TimeHarp 200, from PicoQuant GmbH (Berlin, Germany) to record the fluorescence decays. The fluorescence decays shown correspond to a total acquisition time of ∼2000 s.

Synthesis of Polyproline Donor−Acceptor Constructs. Donor (**D**) only, acceptor (**A**) only, and doubly labeled (**DA**) peptides were synthesized in house. Rhodamine 575 was coupled to the side chain of the C-terminal lysine residue and used as the donor fluorophore, while Rhodamine 640 was attached to the N-terminus of peptides and acted as the acceptor. All peptides were capped with a C-terminal amide and donor-only peptides were capped on the N-terminus by an acetyl group (Ac). The polyproline peptides $GlyGlyPro_8Lys$ and $GlyGlyPro_{14}Lys$ were synthesized by microwave-assisted solid-phase peptide synthesis on a 0.1 mmol scale using Fmoc-protected amino acids and rink amide resin as the solid support. Following peptide synthesis, the acceptor fluorophore (for **A**- and **DA**-labeled peptides) was coupled through an amide linkage to the free N-terminus of the peptide while it was still linked to the resin. An activated version of Rhodamine 640, 5-carboxy x-rhodamine succinimidyl ester (Anaspec, Inc., Fremont, CA) was used for the coupling. The peptides were cleaved from the solid support using 95% trifluoroacetic acid (TFA)/2.5% thioanisole/2.5% H_2O and purified by analytical reverse-phase C18 high-performance liquid chromatography (HPLC) using an acetonitrile/H_20 (0.1% TFA) gradient of 5−100% acetonitrile, over 60 min. The donor fluorophore was coupled in solution through an amide linkage made to the side chain of the C-terminal lysine residue. 5-Carboxy-rhodamine 6G succinimidyl ester (an activated form of Rhodamine 575 obtained from Anaspec) was used for donor labeling. All dye coupling reactions used ∼6-fold excess dye in dimethylformamide (DMF)/*N*,*N*-diisopropylethylamine (DIPEA). The constructs were again purified by reverse-phase HPLC. MALDI time-of-flight analysis as well as ESI-Fourier transform ion cyclotron resonance mass spectrometry gave peaks at the expected mass-to-charge ratios for each construct, although proline deletion products, uncoupled dye, and incompletely labeled peptides were also present in the sample. Fortunately, these appear at different mass-to-charge ratios and could be effectively ejected from the trapped ion population during the gas-phase experiments.

Polyproline synthesis exceeding approximately seven prolines in tandem resulted in a progressive decrease in coupling efficiency

(34) Watkins, L. P.; Chang, H.; Yang, H. *J. Phys. Chem. A* **2006**, *110*, 5191–5203.
(35) Dolghih, E.; Ortiz, W.; Kim, S.; Krueger, B. P.; Krause, J. L.; Roitberg, A. E. *J. Phys. Chem. A* **2009**, *113*, 4639–4646.
(36) Schuler, B.; Lipman, E. A.; Steinbach, P. J.; Kumke, M.; Eaton, W. A. *Proc. Natl. Acad. Sci. U.S.A* **2005**, *102*, 2754–2759.
(37) Shi, X.; Duft, D.; Parks, J. *J. Phys. Chem. B* **2008**, *112*, 12801–12815.
(38) Counterman, A. E.; Clemmer, D. E. *J. Phys. Chem. B* **2004**, *108*, 4885–4898.
(39) Danell, A.; Parks, J. H. *Int. J. Mass Spectrom.* **2003**, *229*, 35–45.
(40) Dashtiev, M.; Azov, V.; Frankevich, V.; Scharfenberg, L.; Zenobi, R. *J. Am. Soc. Mass Spectrom.* **2005**, *16*, 1481–1487.
(41) Forbes, M. W.; Talbot, F. O.; Jockusch, R. A. In *Practical Aspects of Trapped Ion Mass Spectrometry: Applications of Ion Trapping Devices*; March, R. E., Todd, J. F. J., Eds.; CRC Press: Boca Raton, FL, 2009; Vol. 5, Chapter 9, pp 239−290.

and increasing amounts of proline deletion products. Due to these difficulties, synthesis of the GlyGlyPro_{20}Lys peptide was carried out manually using rink amide resin and Fmoc-protected amino acids as described above. Briefly, reaction sequences were composed of deprotection, activation/coupling, and capping steps. The rink amide resin was initially swelled in dichloromethane (DCM) for 10 min prior to Fmoc deprotection. Deprotection steps were carried out using 20% piperidine/DMF for 1 h at room temperature, followed by extensive DMF washes. Coupling was accomplished using ~6-fold excess of each proline and 2-(1*H*-7-azabenzotriazol-1-yl)-1,1,3,3-tetramethyl uronium hexafluorophosphate methanaminium (HATU) in DMF/DIPEA for 2−3 h periods at room temperature. Following extensive DMF washes, unreacted prolines were capped using 20% acetic anhydride/1% DIPEA/*N*-methyl-2-pyrrolidone (NMP) for 1 h at room temperature. The beads were again washed several times with DMF, and the cycle was repeated. Fluorophore coupling and deprotection off the solid support were done as described above for the Pro_8- and Pro_{14}-based peptides. The Pro_{20}-based peptides were less soluble in water than the shorter peptides; therefore, a 20% DMF/H_2O solution was used to solubilize the construct prior to HPLC injection. Reverse-phase HPLC was used to purify the samples, and their identities were checked using MALDI and ESI mass spectrometry.

Modeling. A molecular mechanics conformation searching strategy was used to explore the complex potential energy surfaces of the dye-labeled peptides. Starting structures with different charge configurations and peptide bond angles were built using the Maestro interface, and conformation searching was performed using MacroModel v. 8.5 (both from Schrodinger, LLC. Portland, OR). Conformation searches with the Merck molecular force field (MMFF94s) of at least 3000 steps per starting structure were performed using the Monte Carlo multiple minimum (MCMM) method implemented in MacroModel. No constraints were applied during the MCMM search.

While each dye should be charged, it is not clear where the remaining charges are located on each peptide. Thus, isomers with different sites of protonation were constructed as follows. All isomers modeled had charges located on both dyes. For the 3+ charge state of the $n = 14$ peptide, the third charge was placed on the nitrogen located on either Pro4, Pro7, Pro10, the C-terminal amide, or the lysine side chain to which the (charged) donor dye is coupled. This produced five different isomers, the initial structures of which had all peptide bonds in the trans ($\omega = 180°$) configuration.

Eight different starting configurations of the 4+ charge state of the $n = 14$ peptide were constructed. Four of these started with an all-trans peptide bond configuration with the third and fourth charges placed on nitrogens located at (Pro4, Pro10), (C-terminal amide, Pro4), (C-terminal amide, Pro7), or (C-terminal amide, Pro10). Four structures for the 4+ charge state of the $n = 14$ peptide which started with cis ($\omega = 0°$) geometries of the proline peptide bonds were also explored. Two of these had additional charges on either (Pro4, Pro10) or (C-terminal amide, Pro4). The remaining two starting structures were protonated on the nitrogen of the C-terminal amide and the carbonyl oxygen of either Gly1 or Pro10.

For the 5+ charge state of the $n = 14$ peptide, just two starting structures were used for MCMM conformation searches. These both featured all-trans peptide bonds and protonation on either dye and on the nitrogens of (Pro2, Pro7, Pro13) and (Pro4, Pro10, C-terminal amide).

The potential energy surface of these peptides is complex, and the conformation searching employed was not exhaustive. Thus, the searches may not have identified the most stable structure(s) for each molecule. However, the range of structures identified with this procedure should provide at least a reasonable representation of the conformational space available to each molecule.

Results and Discussion

Steady-State Spectra. While many donor−acceptor pairs have been characterized for FRET experiments in solution, spectroscopic data for gaseous ions are sparse. Furthermore, spectral properties may differ dramatically between solution and gas phase. This observation forced us to re-examine in the gas phase the spectroscopic properties of several conventional dyes.[27,42] Following these investigations, we selected two Rhodamine dyes that constitute a suitable FRET pair in the gas phase. Figure 1 shows the excitation and emission spectra recorded for Rhodamine 575 (Rh575, the donor, also known as Rhodamine 19, which is a free acid variant of the better known Rhodamine 6G) and Rhodamine 640 (Rh640, the acceptor, also known as Rhodamine 101). Due to the limited tunability ($\lambda < 540$ nm) of our laser, only a partial excitation spectrum of the acceptor could be recorded. This partial spectrum is however sufficient to ascertain the good spectral overlap between the two dyes and to estimate the Förster distance (R_0) associated with that dye pair (see below). The donor was attached to the side-chain of the lysine residue on the C-terminal end of the peptide while the acceptor was coupled to the N-terminus. The FRET-pair-labeled peptides thus formed have the general formula **A**-Gly-Gly-Pro_n-Lys(**D**)-NH_2 where *n*, the number of proline residues, is equal to 8, 14, and 20.

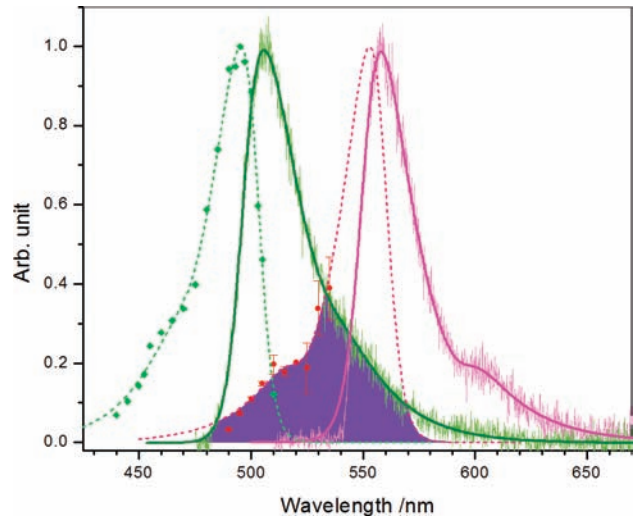

Figure 1. Fluorescence excitation (solid symbols) and emission (thin line) spectra of the donor (Rh575, green) and acceptor (Rh640, red) dyes chosen for FRET. The thick solid and dashed lines are least-squares fits of the data with double sigmoidal functions (see the text). The shaded area shows the spectral overlap for these two dyes.

Upon electrospray ionization of the sample, multiple charge states of each peptide were observed in the mass spectra. For the doubly tagged peptide (donor and acceptor) of the $n = 14$ peptide, these corresponded to the $[M + 3H]^{5+}$ at *m*/*z* 516, $[M + 2H]^{4+}$ at *m*/*z* 645, and $[M + H]^{3+}$ at *m*/*z* 859.5. These species could be isolated in the QIT to a sizable population of at least 30 000 ions (ICC ~ 600 000). Similar ion populations were also isolated for the singly tagged peptides.

The steady-state fluorescence spectra of the isolated Pro_{14}-based peptides are shown in Figure 2. The charge states shown each carry two protons on the peptide, in addition to the charged dyes. Upon excitation at 470 nm, the singly tagged donor−peptide Ac-GlyGlyPro_{14}Lys(**D**)-NH_2 shows a strong emission with a maximum at 518 nm (Figure 2b), shifted by 14 nm to the red compared to the bare Rhodamine 575 dye, isolated in the gas phase (Figure 1).[42] A similar red shift of ~7 nm is also observed

(42) Forbes, M. W.; Jockusch, R. A. *J. Am. Soc. Mass Spectrom.* **2010**, in press.

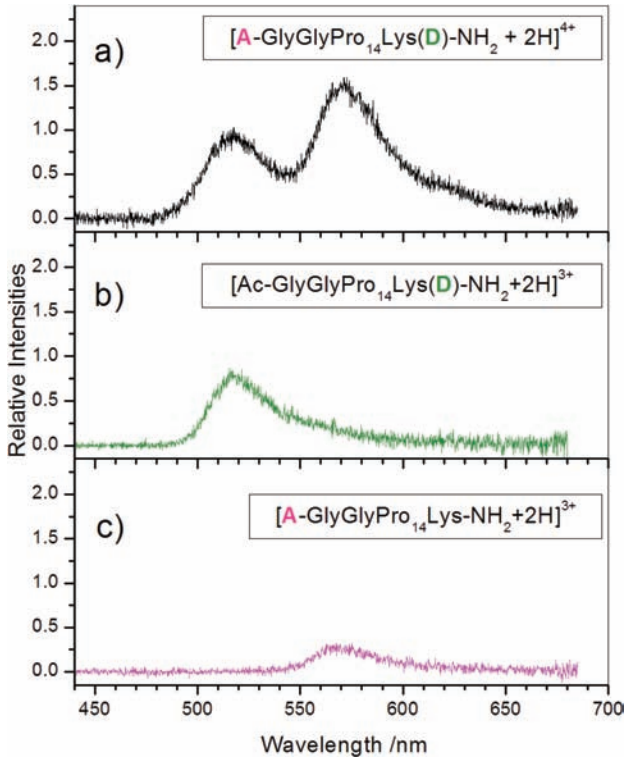

Figure 2. Emission spectra of Pro_{14}-based peptides containing (a) both donor and acceptor, (b) only the donor, and (c) only the acceptor. All spectra are normalized by ion population, laser power, and integration time.

for the acceptor-only peptide **A**-GlyGlyPro$_{14}$Lys-NH$_2$ compared to the isolated dye molecule. These red shifts could be attributed to either the different chemical interactions of the dye with the peptide or to the effect of the multiple charges present in the peptide; the latter will be discussed later. Apart from the shift, the spectra of these dyes incorporated in the peptide are identical in shape to that of the isolated molecules. Excitation of the acceptor−peptide at 470 nm yields significantly lower signal (Figure 2c), as expected upon examination of the bare dyes' (albeit partial) excitation spectra in Figure 1. Excitation at 520 nm, however, leads to a much stronger emission, confirming that the dye's spectroscopic properties were slightly red-shifted upon attachment to the peptide.

Figure 2a shows the emission spectrum of the donor−acceptor peptide, excited at 470 nm. Two distinct bands are observed: one centered around 518 nm, corresponding to emission from the donor and the other, centered around 572 nm, corresponding to emission from the acceptor. Comparison of the intensities observed in the three spectra in Figure 2 shows without any ambiguity that FRET is taking place. The intensity of the acceptor band is much larger than that of the acceptor-only peptide, indicating sensitized emission from the acceptor.

Fluorescence Lifetimes. FRET provides an additional decay channel to the excited donor molecules, which must be reflected by a decrease in their fluorescence lifetime. This decrease in lifetime provides a route to measure FRET efficiencies that is more reliable than steady-state intensities.

In order to measure only the lifetime of the donor within the DA-labeled peptide, a band-pass filter was placed in the collection path to ensure that only light from the donor reaches the SPAD detector (see Figure S1 in Supporting Information). Figure 3 shows the measured decays for the donor in both the donor-only (panel a) and donor−acceptor (panel b) peptides with

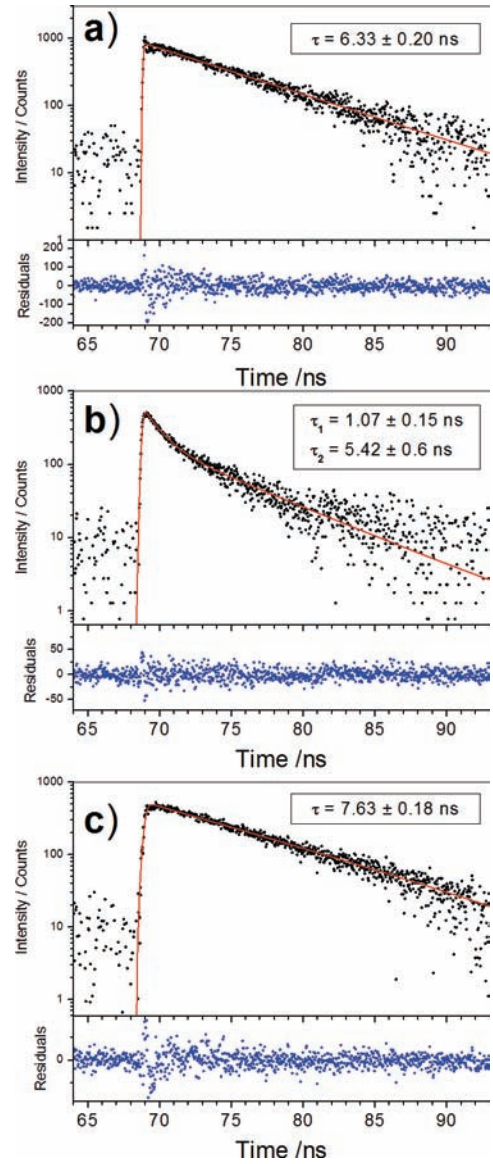

Figure 3. Fluorescence decays and fitted lifetimes for (a) the donor in the [Ac-GlyGlyPro$_{14}$Lys(**D**)-NH$_2$+2H]$^{3+}$ peptide, (b) the donor in the [**A**-GlyGlyPro$_{14}$-Lys(**D**)-NH$_2$+2H]$^{4+}$ peptide, and (c) the acceptor in the [**A**-GlyGlyPro$_{14}$-Lys(**D**)-NH$_2$+2H]$^{4+}$ peptide.

the corresponding fits by exponential decays convoluted with a Gaussian detector response function. Visual inspection is enough to establish that the donor's lifetime is considerably decreased in the presence of the acceptor. The decay of Rh575 in the donor-only peptide is well-fit by a single exponential with lifetime of 6.33 ± 0.18 ns, slightly longer than that of the isolated gaseous dye of 5.7 ± 0.2 ns.[43] Similarly, the lifetime of the acceptor (Rh640) in the donor−acceptor peptide was found to be 7.63 ± 0.18 ns, also slightly longer than the lifetime of the bare Rh640 of 7.0 ± 0.2 ns.[43] Fitting the decay of the donor in the donor−acceptor peptide with a single exponential was not possible as clear oscillations were visible in the residuals. Upon addition of a second decay component, a good fit of the experimental data (see figure 3b) was obtained. The two fitted lifetimes are widely spaced. This strongly suggests

(43) Nagy, A.; Talbot, F. O.; Czar, M. F.; Jockusch, R. A. In preparation, 2010.

the presence of (at least) two distinct populations (or families of populations) of the peptide that exhibit different extents of FRET.

In the simplest interpretation, the two fitted lifetimes are associated with two distinct conformational families of the peptide, and the fitted fractional amplitudes correspond to their relative populations. Using this interpretation, the larger population (fitted fractional amplitude of 0.66) exhibits a lifetime of 1.07 ± 0.15 ns, corresponding to an energy transfer efficiency $E = 1 - \tau_{DA}/\tau_D \simeq 0.83$ (~83%), which indicates a close proximity of the two dyes. The second population shows a lifetime of 5.4 ± 0.6 ns, corresponding to a less efficient energy transfer (~14%) and is consistent with a larger dye−dye separation. This result is promising, as it shows the ability of FRET to identify the presence of multiple conformations within an ensemble of gaseous ions. However, we cannot rule out, on the basis of the present analysis, the presence of a more complex conformational ensemble in our experiments.

There are at least two general cases that can give rise to a double population: the first one is the presence, in the trap, of two species sharing the same R_0 value but with different dye−dye separations. Another possibility is the presence of two populations having distinct R_0 values, which could occur if at least one of the two dyes is not freely rotating. In order to evaluate the distance between the two fluorophores, an estimate of the Förster distance, R_0, for these two dyes is necessary.

Estimation of R_0. According to Förster formalism, the energy transfer efficiency, E, and the dye−dye distance, r, are related by

$$E = \frac{1}{1 + \left(\frac{r}{R_0}\right)^6} \tag{1}$$

The Förster distance R_0 is the distance at which the energy transfer efficiency is 50%. It can be calculated using the spectroscopic properties of the two dyes[1] and is given by the equation

$$R_0 = \sqrt[6]{\frac{9000 \ln(10)}{128\pi^5 N_A}\frac{\kappa^2 \phi_D J}{n^4}} \tag{2}$$

where N_A is Avogadro's number; ϕ_D is the donor's quantum yield in the absence of the acceptor, n is the index of refraction of the medium (1 in our case), κ^2 is the orientation factor, and J is the spectral overlap integral of the donor−acceptor pair. Because the trapped ion population is extremely low, we are not able to measure the actual gas-phase absorbance and quantum yield of the dyes. Moreover, these data are not available in the literature, possibly because the ionic nature of these dyes precluded the use of traditional vaporization methods. We must therefore make several estimations of gas-phase parameters in order to evaluate R_0. The orientation factor was taken as $\kappa^2 = 2/3$, which assumes free rotation of the dyes within their fluorescence lifetimes. We are fully aware that the tethered nature of the dye, in such experiments, may reduce the rotational flexibility of the dye. However, unless κ^2 is close to 0, the error in the estimation of R_0, due to this approximation, is expected to be below 30%.[1] Further measurements of the anisotropy decays of the dyes' fluorescence are planned in our laboratory in order to assess the validity of this assumption for κ^2.

Approximations were also needed in order to calculate the spectral overlap integral because only a partial measurement of the acceptor's excitation spectrum is available. A mirror image of the fitted emission spectrum, modified to allow compression of its width and variable position of the band maximum, was used as a fitting function for the partial excitation spectrum data (Figure 1). This assumption seems reasonable given that we have observed such mirror image symmetry between emission and excitation spectra for several gaseous Rhodamine dyes.[42] The fitted analytical functions thus obtained for both emission of donor and excitation of acceptor are shown in Figure 1. These were then used to calculate the overlap integral as

$$J = \int_0^\infty F_D(\lambda)\, \varepsilon_A(\lambda)\lambda^4\, d\lambda \tag{3}$$

where $F_D(\lambda)$ is area-normalized and $\varepsilon_A(\lambda)$ is the fitted, amplitude-normalized absorbance spectrum of the acceptor, multiplied by the estimated gas-phase molar absorptivity of the acceptor. The gas-phase molar absorptivity is estimated using the empty elliptical cavity model,[44] yielding

$$\varepsilon_{soln}(\lambda) = \frac{n^3}{[(1 - L_\mu)n^2 + L_\mu]^2}\varepsilon_0(\lambda) \tag{4}$$

where ε_{soln} and ε_0 are the molar absorptivities in the solvent and in vacuum, respectively, and n is the solvent's index of refraction. The molar absorptivity of Rh640 in ethanol[45] (95 000 M^{-1} cm^{-1}) was used for the calculation. L_μ is equal to 1/3 for the spherical cavity. Using these values results in a decrease in molar absorptivity of the acceptor of ~2.5%.

The same formalism was used to evaluate the gas phase quantum yield of the donor, Rh575; this model links the gas- and solution-phase radiative rates Γ by

$$\Gamma_{soln} = \frac{n^5}{[(1 - L_\mu)n^2 + L_\mu]^2}\Gamma_0 = n^2\frac{\varepsilon_{soln}(\lambda)}{\varepsilon_0(\lambda)}\Gamma_0 \tag{5}$$

where Γ_0 is the gas-phase radiative rate. Using this relationship, the ratio of the gas-phase and solution-phase quantum yield can be written as

$$\frac{\phi_0}{\phi_{soln}} = \frac{\Gamma_0}{\Gamma_{soln}}\frac{\tau_0}{\tau_{soln}} = \frac{1}{n^2}\frac{\varepsilon_0(\lambda)}{\varepsilon_{soln}(\lambda)}\frac{\tau_0}{\tau_{soln}} \tag{6}$$

Using the reported value of the quantum yield and lifetime of Rh575 cation in ethanol,[46] the spherical cavity model estimate for the change in molar absorptivity upon transfer to the gas phase ($\varepsilon_0/\varepsilon_{soln}$), τ_0 of 5.7 ns,[43] and the index of refraction for ethanol (1.3611), the quantum yield of the donor in the gas phase is estimated to be $\phi_0 \sim 0.65$, which is somewhat lower than Rh575's measured quantum yield in ethanol but similar to that in water.[46] With these assumptions, the calculated overlap is $J \sim 2.39 \times 10^{15}$ M^{-1} cm^{-1} nm^4, leading to an estimate of $R_0 \sim 67$ Å. This calculated Förster distance of 67 Å for our dye pair would therefore suggest that the two observed lifetimes (1.1 and 5.4 ns) in the donor−acceptor peptide correspond to two conformers having dye−dye distances of 51 and 90 Å, respectively. The larger distance of 90 Å is clearly too high, as the maximum dye−dye distance found in all our MMFF

(44) Toptygin, D. *J. Fluoresc.* **2003**, *13*, 201–219.
(45) Brackmann, U. Lambdachrome laser dyes, 1986.
(46) López Arbeloa, T.; López Arbeloa, F.; Hernández Bartolomé, P.; López Arbeloa, I. *Chem. Phys.* **1992**, *160*, 123–130.

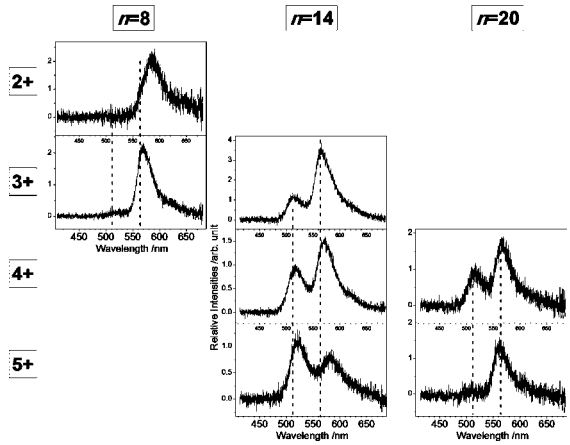

Figure 4. Influence of charge states on the emissions of **A**-GlyGlyPro$_n$Lys(**D**)-NH$_2$ peptides of various lengths: $n = 8$ (left), 14 (middle), and 20 (right) prolines. The pink (564 nm) and green (512 nm) dashed lines are guides for the eyes to illustrate the shifts in band position of the various species.

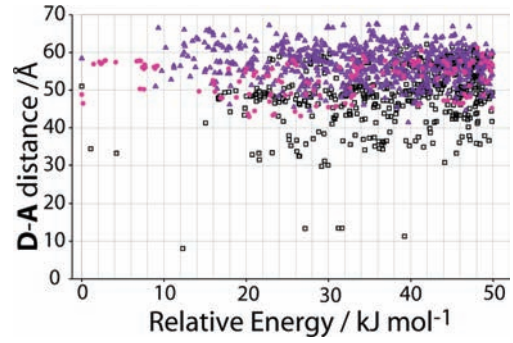

Figure 5. Donor−acceptor distances for computed MMFF conformations of the **A**-GlyGlyPro$_{14}$Lys(**D**)-NH$_2$ peptide for the 3+ (black squares), 4+ (magenta circles), and 5+ (purple triangles) charge states. Conformations were identified from a Monte Carlo multiple minimum conformation search starting with all peptide bonds in trans-configuration. The distance shown is between the central oxygens of each dye. Charges are located on the acceptor dye, the donor dye, and on the nitrogens of 3+ (Pro7), 4+ (Pro4, Pro10), and 5+ (Pro2, Pro7, Pro12) charge states.

simulations (over 25 000 structures) was 71 Å. Note that R_0 is proportional to the sixth root of the *product* of our three estimated quantities (namely ϕ_D, ε_0, and κ^2). If the numbers above overestimate this product by a factor of 6, for example, R_0 would be too high by $\sqrt[6]{6} \approx 1.3$-fold, which would reduce R_0 from 67 to 50 Å. A better determination of R_0 for this FRET pair requires further experiments using more rigid gas-phase "molecular rulers." At present, further insight into the value of R_0 is sought using comparison with molecular mechanics calculations (see below).

Peptide Length and Charge State. The electrospray process forms multiple charge (protonation) states for molecules of sufficient size. This enables investigation of the effects of Coulomb repulsion on peptide conformation. Figure 4 illustrates the impact of peptide length (containing 8, 14, and 20 prolines) and charge state on the recorded emission spectra. As expected, the shorter Pro$_8$-based peptide shows almost no fluorescence from the donor, indicating that energy transfer is virtually complete, consistent with a substantially shorter dye−dye distance than in Pro$_{14}$-based peptides. No change in FRET efficiency is observed, as both available charge states (2+ and 3+) showed complete energy transfer.

For the longer Pro$_{14}$-based peptides (middle column, Figure 4), bands corresponding to both donor and acceptor fluorescence are observed, and charge state has a clear effect: FRET efficiency decreases with increasing number of charges. This is consistent with the adoption of more extended conformation in peptides with greater Coulombic repulsion. Note as well the monotonic red shifts (~4 nm shift with each additional charge) of the dyes' emission maxima with increasing number of charges in the peptide.

Interestingly for the $n = 14$ peptide series (Figure 4, middle column), it appears that the donor band intensity does not change significantly with charge state, while the acceptor band intensity is dramatically altered. This may simply be a consequence of less efficient excitation with 470 nm light as the charge state increases, as suggested by the red-shift in emission. It may also be that using the recorded ICC value as a proxy for ion number in our normalization procedure introduces a systematic error; i.e., if the ion detector is more sensitive to higher charge state ions, then at a given ICC value, fewer high charge state ions will be trapped, resulting in lower apparent total fluorescence signal from the higher charge states. Additional experiments are underway to further examine the cause(s) of this phenomenon.

The $n = 20$ peptides show unexpected results (Figure 4, right-hand column). The chain length is substantially longer than that of the $n = 14$ peptide; however, the 4+ charge states exhibit similar extents of FRET, suggesting that dye−dye distances in the 4+ charge state of the Pro$_{14}$- and Pro$_{20}$-based peptides are similar. Furthermore, addition of a fifth charge results in virtually complete energy transfer, suggesting the close proximity of the two dyes. This could result if the peptide adopts a hairpin-type structure in which the ends are brought close together. Clearly, these peptides do not simply exist as rigid rods (such as polyproline I or II helices) of extendible length. This observation is in agreement with recent single molecule solution studies by Schuler et al.[5] and ion mobility experiments on gaseous polyprolines by Counterman and Clemmer.[38]

We note that the isolated populations of the $n = 20$ peptide was smaller than those of the $n = 14$ peptide by a factor of 2−3. This was due, at least in part, to signal suppression in the ESI because of a substantial amount (over 99% of the MS signal) of uncoupled dye in solution. The lower signal-to-noise ratio of the $n = 20$ spectra is a consequence of the smaller number of ions probed. Interestingly, this also illustrates the advantage of the controlled environment of a mass spectrometer, as such a level of contamination would make FRET measurements in solution almost impossible while only reducing the sensitivity of these gas-phase experiments.

Another remarkable feature is the direction and magnitude of the spectroscopic shift in emission with increasing number of charges on the peptides. As mentioned earlier, a systematic red shift of ~4 nm is observed for the $n = 14$ peptide. However, the reverse is observed for the $n = 8$ and 20 peptides, which both display *blue* shifts in the acceptor band as the charge increases. While the magnitude of these shifts is similar for the $n = 14$ and 20 peptides (4−6 nm), the shift is about 4 times higher in the $n = 8$ peptide (18 nm). This magnitude and direction of the spectral shift could well provide some insight into the position of the charges in the peptide. However, extracting this information is not straightforward, as the influence of electric fields on the spectroscopy of chromophores is complex.[47,48]

Molecular Mechanics Conformations. The conformational landscape of these large dye-labeled peptides is complex.

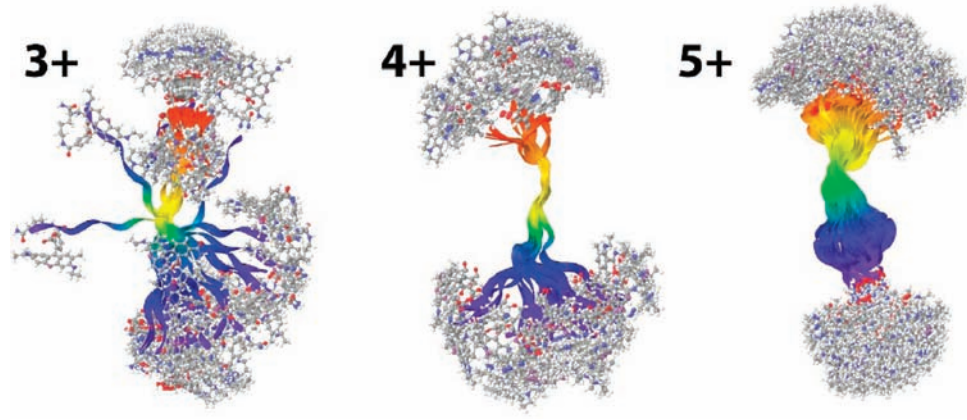

Figure 6. Superposition of MMFF conformations found within 30 kJ/mol of the most stable structure identified for **A**-GlyGlyPro$_{14}$Lys(**D**)-NH$_2$ for the 3+, 4+ and 5+ charge states. The peptide backbone is represented as a ribbon changing from red (N-terminus) to blue (C-terminus). The donor and acceptor dyes are shown in a ball-and-stick representation.

Conformational searching with the MMFFs was used to explore their potential energy landscape. Figure 5 shows the effect of charge state on calculated donor−acceptor distances as a function of relative energy for a subset of the conformations identified for the $n = 14$ based peptides. The series shown has charges located on both dyes and on proline nitrogens evenly spaced along the backbone, i.e., on Pro7 for the 3+ charge state, on Pro4 and Pro10 for the 4+ charge state, and on Pro2, Pro7, and Pro12 for the 5+ charge state. Figure 6 shows a superposition for each charge state of all structures identified within 30 kJ mol^{-1} of the minimum. As can be seen from both Figures 5 and 6, the 4+ and 5+ charge states are quite extended, with donor−acceptor distances of conformations within 10 kJ mol^{-1} of the minima ranging from 46 to 56 Å for the 4+ structures and from 51 to 67 Å for the 5+ structures. In contrast, both relatively extended and more compact conformations of low energy were identified for the 3+ peptide; the donor−acceptor distance in the most stable 3+ conformation found is 51 Å, while just 1 kJ mol^{-1} higher in energy is a bent conformation, which has a donor−acceptor distance of just 34 Å. While an exhaustive search of the conformational energy landscape has not been performed, the results shown here are in qualitative agreement with the FRET spectra shown for the $n = 14$ peptide in Figure 4. That is, as the charge state of the peptide increases, the peptide becomes more extended, increasing the average distance between the donor and acceptor moieties.

Of the eight different configurations examined with conformation searching for the $n = 14$, 4+ peptide (see methods), the longest donor−acceptor distance found was 68 Å for conformations lying within 50 kJ mol^{-1} relative to the minimum for each charge configuration. This suggests that the conformer showing the least FRET (14% from lifetime measurements) should have dyes which are less than 68 Å apart. Using these values in eq 1, an upper limit for R_0 of 50 Å is estimated. Using this value of R_0 to estimate the dye−dye distance for the other conformer, which had 83% transfer efficiency, results in a computed dye−dye separation of 39 Å. This is 15% shorter than the calculated shortest distance for the 4+ state of the $n = 14$ peptide shown in Figures 5 and 6 (46 Å) but matches well the distance computed for low-energy conformers based on a PPI helix (40 Å; see Figure S3, Supporting Information). We are currently performing quantum mechanical geometry optimizations on some selected conformations from the MMFF simulations in order to better assess relative energies of different conformations and the accuracies of the dye−dye distances provided by the force-field.

Conclusions and Perspectives

We have measured the dispersed fluorescence and fluorescence decays of polyproline peptides tagged with a pair of dyes selected for gas-phase FRET. Three different lengths of peptides containing 8, 14, and 20 prolines were investigated. Fluorescence energy transfer was evidenced by the spectral profiles of fluorescence emissions and quantified by measuring the fluorescence lifetime of the donor dye with and without the acceptor dye attached to the peptides. Virtually complete energy transfer is observed for the peptides containing eight prolines. For the peptide containing 14 prolines, the presence of at least two distinct populations (conformers or conformational families) showing different amounts of energy transfer was revealed, illustrating the usefulness of FRET in probing gas-phase conformations. The longer peptide, with 20 prolines, showed highly efficient energy transfer not compatible with the extension of a rigid helical structure. The high FRET efficiency observed in these peptide suggests a bent structure that brings the two dyes in close proximity. Multiple charge states of each peptide were individually isolated and investigated. FRET efficiency decreased with increasing charge state of the $n = 14$ peptide, consistent with Coulombic repulsion favoring a more extended structure.

Qualitative information (relative dye−dye distances) is readily accessed from FRET results. However, significant work remains to be done. Better characterization of the Förster distance for dye pairs in the gas phase is needed to improve the accuracy of the extracted dye−dye distances. The lack of data on *gas-phase* absorbance is a significant hurdle. To circumvent this, a stiff "molecular ruler", of known length, must be used for distance calibration. Polyproline peptides are clearly too flexible for this purpose. One must also consider the effect of charges on the attached dyes' spectroscopic properties, as these properties have a direct impact on R_0. Spectral measurements must be correlated to changes in fluorescence lifetime, which are generally viewed as a more robust reporter of FRET. In addition, alternative dye pairs must be explored; dyes that are not intrinsically charged may be a better choice for future FRET studies, as the charged

(47) Philip, A. F.; Nome, R. A.; Papadantonakis, G. A.; Scherer, N. F.; Hoff, W. D. *Proc. Natl. Acad. Sci. U.S.A* **2010**, *107*, 5821–5826.
(48) Boxer, S. G. *J. Phys. Chem. B* **2009**, *113*, 2972–2983.

dyes may influence more strongly the preferred conformations of the peptide backbone.

This work presents fluorescence spectra and lifetime measurements showing gas-phase FRET, thus opening a new route to probe the conformation of gaseous molecules. The use of this sensitive spectroscopic technique in combination with the controlled environment of a mass spectrometer will also enable investigation of the connection between solution and gas-phase properties of large biomolecules through the study of clusters containing a well-defined number of solvent molecules. Similar to experiments now routinely done in solution, we envision the use of FRET to monitor protein conformation and dynamics as a function of ligand binding or protein−protein interaction. Performing these experiments as a function of temperature will provide valuable information about the flexibility and thermodynamics of the investigated biomolecules, both alone and within complexes.

Acknowledgment. Funding from the Canada Foundation for Innovation, the Ontario Research Fund, the Canada Research Chairs program, and the Natural Sciences and Engineering Research Council of Canada is gratefully acknowledged.

Supporting Information Available: Scheme of synthesized peptides; emission spectra showing the filtering method that allowed measurements of the individual fluorescence of donor and acceptor in the doubly tagged Pro_{14} peptide; low-energy conformers of 4+ charge state of Pro_{14}-based peptide, identified using conformation searching. This material is available free of charge via the Internet at http://pubs.acs.org.

JA1067405